GENES, CHROMOSOMES & CANCER 28:258–268 (2000)

Genetic Analysis of the *APAF1* Gene in Male Germ Cell Tumors

Shashi Bala[1], Holt Oliver[2], Beatrice Renault[3], Kate Montgomery[3], Shipra Dutta[1], Pulivarthi Rao[4], Jane Houldsworth[4], Raju Kucherlapati[3], Xiaodong Wang[2], R.S.K. Chaganti[4], and V.V.V.S. Murty[1]*

[1]Department of Pathology, College of Physicians & Surgeons of Columbia University, New York, New York
[2]Department of Biochemistry, University of Texas Southwestern Medical Center at Dallas, Dallas, Texas
[3]Department of Molecular Genetics, Albert Einstein College of Medicine, Bronx, New York
[4]Laboratory of Cancer Genetics and the Department of Human Genetics, Memorial Sloan-Kettering Cancer Center, New York, New York

Cytogenetic and molecular analyses have shown that the chromosome band 12q22 is recurrently deleted in male germ cell tumors (GCTs), indicating the presence of a candidate tumor suppressor gene (TSG) in this region. To identify the TSG, we mapped the *APAF1* gene, a proapoptotic mammalian homologue of *ced-4*, to chromosomal band 12q22, that suggested that this might be the candidate deleted gene in GCTs. We further localized the gene between the polymorphic markers D12S1671 and D12S1082 at 12q22 to determine the role of *APAF1* in the pathogenesis of GCT, and we characterized its normal genomic structure and analyzed its alterations in GCTs. The *APAF1* gene comprises 27 exons, with the coding region spanning 26. The region containing *APAF1* was found to be deleted in GCT by fluorescence in situ hybridization analysis, but without evidence of coding sequence alterations. RT-PCR and Western blot analysis showed *APAF1* gene expression at detectable levels in all GCT cell lines analyzed. An aberrant-sized APAF1 protein was seen in one cell line. This and 2 other cell lines carrying *APAF1* deletions also exhibited defects in dATP-mediated caspase-3 activation. Caspase-3 activity was effectively restored by addition of recombinant caspase-9 and APAF1 proteins, and to a lesser extent by caspase-9 alone, but not by APAF1 alone. These data do not support a TSG role for *APAF1*, but defects in other components of the apoptotic pathway that may be related to 12q22 deletion cannot be ruled out. *Genes Chromosomes Cancer 28:258–268, 2000.*

INTRODUCTION

Cytogenetic and molecular genetic studies on male germ cell tumors (GCTs) have identified alterations affecting both the short and the long arms of human chromosome 12 (Chaganti et al., 1996). Cytogenetic studies have identified deletions affecting 12q or monosomy of 12q in a high proportion of GCTs (Murty et al., 1990; Samaniego et al., 1990; Rodriguez et al., 1992). At the molecular genetic level, restriction fragment length polymorphism (RFLP) studies identified loss of heterozygosity (LOH) at two sites, 12q13 and 12q22, suggesting the presence of at least two candidate tumor suppressor genes (TSGs) on this chromosomal arm. In addition, homozygous deletion at 12q22 noted in a tumor further supported the view that this region may harbor a candidate TSG (Murty et al., 1992). More recently, fine mapping of 12q22 deletions identified an 830-kb minimal deletion between the markers D12S377 and *P382A8/AG* (Murty et al., 1996, 1999). Similarly, the 12q21-23 region has also been shown to exhibit frequent LOH in pancreatic (Seymour et al., 1994; Hahn et al., 1995; Kimura et al., 1996, 1998) and gastrointestinal (Fey et al., 1989; Schneider et al., 1995) carcinomas. These studies strongly indicated the presence of one or more candidate TSGs at 12q22 that may be involved in the development of GCT and other tumor types.

Genetic studies on the nematode *C. elegans* have identified three genes, *ced*-3, *ced*-4, and *ced*-9, that control the apoptotic cell death pathways, that are conserved in vertebrates including man (Horvitz, 1999). CED-4 is required for development-associated cell death in the worm (Horvitz, 1999). CED-4 interacts physically with CED-3 to mediate proteolytic activation of the immature procaspase CED-3 into enzymatically active forms (Hu et al., 1998; Pan et al., 1998). In this cascade, CED-9 functions upstream of CED-3 and CED-4 by preventing their activation. Mutations that affect CED-4 oli-

Shashi Bala and Holt Oliver contributed equally to this work.

Supported by: Medical Scientist Training Grant (to H.O.); Grant number: GM08014; Robert Welch Foundation (to H.O.); ACS (to X.W.); Grant number: ARE258; NIH (to X.W. and V.V.V.S.M.); Grant numbers: GMRO1-55942, CA75925.

*Correspondence to: V.V.V.S. Murty, Department of Pathology, College of Physicians & Surgeons of Columbia University, 630 West 168th Street, New York, NY 10032. E-mail: vvm2@columbia.edu

Received 17 September 1999; Accepted 30 November 1999

gomerization inactivate its ability to activate the pro-CED-3 molecule and cause it to lose its pro-apoptotic function (Yang et al., 1998). The CED-4 counterpart in man has been identified as APAF1 (Zou et al., 1997). CED-3 is similar to the mammalian caspase-3, whereas CED-9 is homologous to the *BCL2* family of genes. Human *APAF1* mRNA is a 7.2 kb transcript with a 3,582 nt coding region, that encodes a 130 kDa protein (Zou et al., 1997). The first 85 residues of the amino terminal of APAF1 show identity with the amino terminal of CED-3, whereas the following 320 amino acids show similarity with CED-4. The COOH-terminal region lacks homology to CED-4 and is composed of 12 WD-40 repeats. *APAF1*, under the control of *BCL2*, plays a crucial role in cell death pathways through caspase activation. APAF1 has been shown to participate in caspase-3 activation in a cytochrome C-dependent manner (Li et al., 1997; Zou et al., 1997, 1999). Thus, APAF1 functions downstream of CED-9 family members and upstream of CED-3-like caspases in the apoptotic pathway.

Analysis of *Apaf*1-deficient mice exhibited reduced apoptosis in the embryonic brain, leading to overgrowth, hyper-proliferation of neuronal cells, cranio-facial abnormalities, and resistance to various apoptotic stimuli and embryonic death by E16.5 days. Evidently, the *APAF1* gene plays a central role in regulating programmed cell death during mammalian development in mitochondria-dependent apoptosis and is critical for regulation of normal development. Therefore, germline mutations in the gene can lead to abrogation of programmed cell death and developmental defects (Cecconi et al., 1998; Yoshida et al., 1998). Similarly, somatic mutations in *APAF1* and other genes involved in programmed cell death pathways can confer a survival advantage, as exemplified by deletion of the caspase-3 gene in the MCF-7 breast cancer cell line (Janicke et al., 1998). Recently, it has been shown that inactivation of *Apaf1* or caspase-9 has been shown to lead to cellular transformation and tumorigenesis (Soengas et al., 1999). These data suggested that genetic alterations in *APAF1* or the other genes in the pathway disrupt mechanisms of apoptosis and facilitate oncogenic transformation.

In our physical mapping of the 12q22 region, we assigned the *APAF1* gene to the distal border of the minimal deletion in GCT (Murty et al., 1999). In view of its map position and function as a proapoptotic factor, we considered *APAF1* to be a good candidate for the proposed TSG frequently deleted in GCTs. In this study, we report the exact physical map position of *APAF1* and its genomic organization. In a genetic and functional analysis, we also examined the role of *APAF1* in the pathogenesis of GCT and found no evidence in support of a role for this gene.

MATERIALS AND METHODS

Physical Mapping and Identification of Intron-Exon Boundaries

Our previous YAC and high-resolution physical maps of the 12q22 deleted region in GCTs (Murty et al., 1996, 1999; Kucherlapati et al., 1997) have served as a framework in the present mapping studies. During the generation of these maps, we identified several BAC and PAC clones in this region (Murty et al., 1999). We have sequenced ends from a previously mapped PAC clone P373G19 utilizing SP6 and T7 primers and designed nonpolymorphic primer sets for each end (sequences and primer information submitted to GenBank, accession numbers AQ254952 and AQ254953). Probes generated from these ends were utilized for further screening of BAC and PAC libraries (obtained from Dr. Pieter de Jong, Roswell Park Cancer Institute). All of the clones and markers isolated in this manner were placed onto the map by STS-content analysis as described (Murty et al., 1999).

For the identification of the intron-exon boundaries, genomic DNA prepared from a PAC (RPCI3-379G19), and two BAC (RPCI11-396N22 and RPCI11-7L14) clones containing the *APAF1* gene sequences, was utilized as template for sequencing. A panel of 78 overlapping primers in both forward and reverse orientation was designed spanning the entire cDNA sequence. Intronic boundaries identified for exon 18 were based on the KIAA0413E (EST AB007873) sequence. Sequences generated in this manner were compared to cDNA by BLAST searches to identify introns.

Southern Blot Analysis

Southern blot analysis was performed by standard methods after restriction digestion of DNA isolated from P373G19, B396N22, and B7L14 clones. DNAs were subjected to *Eco*RI or *Hin*dIII restriction digestion and transferred to nylon membranes. These blots were hybridized with ^{32}P-labeled *APAF1* cDNA to assess the size of the genomic region.

Cell Lines and Tumor Tissues

Nine GCT cell lines (218A, 169A, 175A, 268A, 287A, 203B, 240A, 228A, and 154A) developed by us (Rodriguez et al., 1992), and the 8 cell lines (Tera-1, Tera-2, 833K-E, 2102E-P, 2102E-R, 2061H, 577M-F, and 577M-lu) provided by Dr. D.L. Bronson (University of Minnesota, MN) were utilized in the present study. All cell lines were cultured in high-glucose DMEM supplemented with 15% fetal bovine serum. In addition, ten primary GCT tumor tissues were utilized (Murty et al., 1994).

Fluorescence In Situ Hybridization (FISH)

FISH was performed by standard methods on normal male metaphase chromosomes and on chromosomes prepared from 8 GCT cell lines. A PAC clone, RPCI3-373G19, containing a part of the *APAF1* gene was biotin-labeled using a bionick-labeling kit (GIBCO/BRL) and was utilized as a probe after suppression with Cot-1 DNA. A Spectrum Orange-labeled chromosome 12 centromeric probe, CEP12 (VYSIS, Downers Grove, IL), was used to enumerate chromosome 12. Double-color FISH was performed, and the biotin-labeled probe was detected with fluorescein-avidin antibody. Fluorescence signals were captured on an Applied Imaging Cytovision Imaging System, and at least 20 metaphase cells were scored under a triple-bypass filter with DAPI counterstain.

Isolation of RNA, Northern Blot Analysis and Multiplex RT-PCR to Evaluate Expression of *APAF1*

Total RNA was isolated utilizing a Stratagene RNA isolation kit according to the manufacturer's protocol. Polyadenylated mRNA was extracted from the frozen cell pellets of at least 2×10^7 cells using Dyna beads (Dynal, Lake Success, NY) according to the manufacturer's protocol. Two micrograms of each mRNA sample was electrophoresed on a 1.2% formaldehyde agarose gel and transferred onto nylon membrane by standard procedures. The membranes were hybridized first with *APAF1* cDNA probe (734 bp of the 5′UTR and 2370 bp of the coding region) followed by a β-actin probe as control. Five micrograms of total RNA was subjected to reverse transcription using random primers and M-MuLV reverse transcriptase (Stratagene, La Jolla, CA) in a 50-μl reaction volume for 60 min at 37°C. Two microliters of the RT reaction product was then subjected to multiplex PCR. The *APAF1* primers (forward 5′-GCTGCCATTTCACCAACAGT-3′ at 2655 bp of cDNA and reverse 5′-CTCTCATTTGCTGATGTCGC-3′ at 2877 bp of cDNA) crossing exons 15 and 16, that yield a 223 bp fragment, combined with β-actin primers that give a 450 bp fragment were utilized for PCR. The PCR products were run on a 1.5% agarose gel and visualized by ethidium bromide staining.

Mutation Screening

SSCP analysis was performed on the entire coding region of the *APAF1* gene in GCTs using 19 overlapping sets of primers derived from the cDNA sequence (Zou et al., 1997). Five micrograms of total RNA extracted from GCT cell lines was reverse-transcribed utilizing random primers in a reaction volume of 50 μl utilizing an RT-PCR kit (Stratagene, La Jolla, CA) according to the manufacturer's protocol. The cDNAs were amplified for 35 cycles of PCR under standard conditions in the presence of 1 μCi of [^{32}P]dCTP (3000 Ci/ml, Amersham, Piscataway, NJ) in a final reaction volume of 25 μl. Diluted PCR products (0.1% SDS/10 mmol/L EDTA and sequencing dye) were heat-denatured and electrophoresed on 6% nondenaturing polyacrylamide gels containing 10% glycerol at room temperature. After electrophoresis, gels were dried and exposed to X-ray film. Autoradiographs were examined for conformational changes. Manual as well as automated sequencing was performed on both strands of purified PCR products of suspected SSCP variants.

Preparation of Cell Extracts

The S-100 cytosolic fraction was prepared from GCT cell lines as described in Liu et al. (1996). Briefly, the cell pellets were suspended in ice-cold buffer A (20 mM HEPES-KOH, pH 7.5, 10 mM KCl, 1.5 mM $MgCl_2$, 1 mM sodium EDTA, 1 mM sodium EGTA, 1 mM dithiothreitol, and 0.1 mM PMSF) by passage through an 18-gauge syringe 12 times. The supernatant from a 20 min centrifugation at 12,000 × *g* was isolated and subjected to 100,000 × *g* in a Sorvall G6-SR ultracentrifuge. The remaining supernatant was collected and the protein concentration determined using the Bradford method.

Western Blot for APAF1

Anti-Apaf1 anti-serum was generated by immunization of rabbits with a recombinant APAF1 fusion protein (see below). One hundred micrograms of the purified proteins, prepared from asynchronous cultures of GCT cell lines extracted by standard methods, were electrophoresed on a 6% SDS-

polyacrylamide gel and then transferred onto BA-S 83 membrane (Schleicher and Schuell, Keene, NH). Immunoblot analysis was performed with a horseradish peroxidase-conjugated goat anti-rabbit (Apaf1) immunoglobulin G using Enhanced Chemi-Luminescence (ECL) Western blotting detection reagents (Amersham, Piscataway, NJ) (Houldsworth et al., 1997; Zou et al., 1997).

Production of APAF1 Fusion Protein

The primers 5′- TCT TCT TCC AGT CAT ATG ACA GTC CTG GTG-3′ and 5′-TTA TGT AGA TCC TGG AGC TCG CTG CAA TTC -3′ were designed to PCR-amplify a segment of the *APAF1* cDNA open reading frame, and the amplified fragment encoding amino acids 101–446 of *APAF1* was sub-cloned inframe into the *Nde*I/*Xho*I sites of the bacterial expression vector pET-15b (Novagen, Madison). The sub-cloned PCR-derived clones were sequenced to confirm that it contained normal cDNA sequence before utilizing in expression studies. The expression plasmid was transformed into bacteria BL21 (DE3). In a typical APAF1 preparation, a 5-ml overnight culture of bacteria containing APAF1 expression vector was added into a 500 ml LB broth, and cultured for 3 hr by shaking at 220 rpm at 37°C. Isopropyl-1-thio-B-D-galactopyranoside (IPTG) was added to the culture at a final concentration of 1 mM with continued shaking for another 2 h. The bacteria were pelleted by centrifugation, and the bacterial pellet was resuspended in 10 ml of buffer B (6 M GuHCl, 0.1 M sodium phosphate, 0.01 M Tris-HCl, pH 8.0). After centrifugation at 10,000 × *g* for 15 min, the supernatant was loaded onto a nickel affinity column (6 ml). The column was washed with 300 ml of buffer B followed by 300 ml of buffer C (8 M urea, 0.1 M sodium phosphate, 0.01 M Tris-HCl, pH 8.0). The column was eluted with buffer C containing 250 mM imidazole.

Assay for Caspase-3 Activation

Caspase-3 was translated and purified as described (Liu et al., 1996). A 2 μl aliquot of the in vitro translated caspase-3 was incubated at 30°C for the indicated time period with a protein fraction in the presence of 1 mM dATP and 1 mM of additional $MgCl_2$ brought to a final volume of 30 μl of buffer A (20 mM HEPES-KOH, pH 7.5, 10 mM KCl, 1.5 mM $MgCl_2$, 1 mM sodium EDTA, 1 mM sodium EGTA, 1 mM dithiothreitol, and 0.1 mM PMSF). At the end of the incubation, 10 μl of 4× SDS sample buffer was added to each reaction. After boiling for 3 min, each sample was subjected to 15% SDS-polyacrylamide gel electrophoresis. The gel was transferred to a nitrocellulose filter that was subsequently exposed to a PhosphorImager plate and visualized in a Fuji BAS-1000 PhosphorImager.

RESULTS

Mapping of *APAF1* Gene Between Polymorphic Markers D12S296 and D12S346

A database search of the sequence obtained from the PAC clone 373G19-T7 mapped to 12q22 identified 169 bp of *APAF1* cDNA sequence, that was subsequently identified as exon 9. Additional screening of PAC and BAC libraries utilizing end sequences generated from P373G19 resulted in identification of 12 additional clones (11 BACs and one PAC). Several existing YACs (Murty et al., 1996) and the clones obtained here were screened for STS content utilizing P373G19 end markers, and 13 previously mapped markers (8 STSs, 3 ESTs, and 2 genes) (Kucherlapati et al., 1997; Murty et al., 1999). An additional primer set generated from the 5′ end of the *APAF1* coding region was also utilized in the analysis. This analysis mapped the *APAF1* gene between the polymorphic markers D12S296 and D12S346 at a 106-cM genetic distance on the chromosome 12 genetic map (Dib et al., 1996) (Fig. 1A). More precisely, *APAF1* is mapped between the loci *TMPO*/*PHC*/D29485 proximally and D12S1218E/D12S1098 distally. This analysis also identified 4 BACs (B396N22, B7L14, B481K9, B313A8) that contained all or most of the 5′ end of the *APAF1* gene, and 9 other clones (B12B10, B170A13, B170I13, B453P16, B548D10, P490A19, P373G19, B14P19, B14P21) that contained all or most of the 3′ end of the gene. The STS-content analysis also determined the transcriptional orientation of the gene from the centromeric to telomeric ends (Fig. 1A).

Intron-Exon Structure of *APAF1*

The overlapping clones P373G19, B396N22, and B7L14 identified by physical mapping containing the entire *APAF1* cDNA sequence were utilized to identify intron-exon boundaries. BLAST comparisons of the generated sequences identified all the intronic boundaries. The *APAF1* gene was found to consist of 27 exons and 26 introns (Table 1, Fig. 1B, GenBank accession Nos. AF098868-AF098914). The coding region of *APAF1* spanned 26 exons, with the translation initiation site (ATG) located at nucleotide position 578 in exon 2, preceded by 5′-UTR within exon 2 and exon 1, and

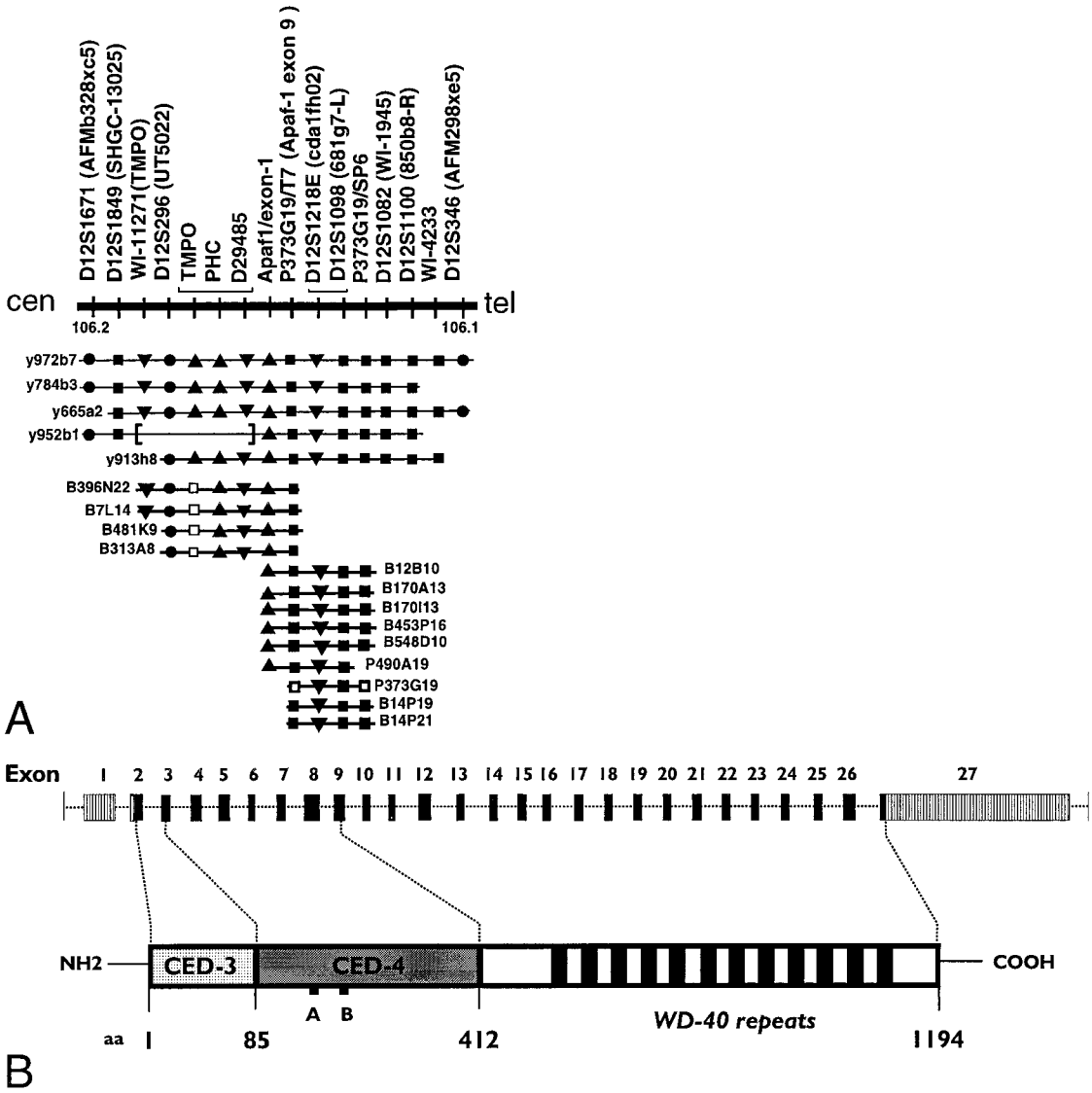

Figure 1. Mapping of *APAF1* gene. (**A**) Physical mapping of *APAF1* gene between polymorphic markers D12S296 and D12S346. The map comprised of 5 YACs (denoted by 'y'), 11 BACs (denoted by 'B'), and 2 PACs (denoted by 'P'). Solid bar on the top represents chromosomal region in centromeric (cen) to telomeric (tel) orientation. The markers placed on the map are shown above the solid bar by vertical lines (distances on the map are not to scale). Thin brackets facing upward indicate that the relative order of the markers could not be determined. Numbers below the solid bar indicate the genetic map positions on chromosome 12. Solid circle, polymorphic marker; solid square, non-polymorphic marker; downward triangle, EST; upward triangle, gene; thin empty square, marker not tested; thick empty square, clone-end marker generated by sequencing of the end. A bracket within a YAC indicates an internal deletion. TMPO, thymopoietin; PHC, phosphate carrier mitochondrial; APAF1, apoptotic protease activating factor-1. (**B**) Schematic representation of genomic organization of *APAF1* gene showing exons and the corresponding protein domains. Black boxes represent coding exons and hatched boxes noncoding exons (drawn to scale) (top), connected by dotted lines as intervening sequences (not drawn to scale). Protein structure at the bottom shows different domains, amino-acid (aa) positions, and their corresponding coding exons by broken vertical lines. A and B in the CED-4 domain indicate consensus sequences for nucleotide binding. Exon 18 represents an alternatively spiced exon resulting in an additional WD 40 repeat (not represented in the figure).

with the 3′ end of the coding region ending at nucleotide position 4159 in exon 27. Exon 27 (3007 bp) encodes the last 49 aa, followed by a large 3′-UTR of 2863 bp (Fig. 1B). Exon 18 represents an alternatively spliced exon, that results in an additional WD repeat in the protein (Zou et al., 1999). We also determined the size of 6 small introns by complete sequencing (Table 1). The *APAF1* gene spans about 55 kb of the genomic region, as estimated from the size of fragments hybridizing to full-length cDNA (data not shown).

Analysis of Mutations and mRNA Expression

We utilized the P373G19 clone to confirm the *APAF1* map position by FISH on normal human metaphase chromosomes. All 30 metaphase cells

TABLE 1. Genomic Organization of APAF-1

Exon	Size (bp)	Intron-5′ **Exon** boundary—3′ **Exon**-intron boundary	Splice acceptor/donor	cDNA location	Intron size
1	536	gat ttg act gtc cgc tgt cca gag gcg gag AAG AAG AGG TAG–GCA AAG GCT TGG gta agt tga cct cct cgc ttt tct ccc cga	AG/GT	1–536	NA
2	179	ctg aca aat att ttg gtg ttt tgg ctg tag CTC ATG GTT GAC–GTA AGA AAT GAG gta aag ctc tct gaa gca gtc cac act tcc	AG/GT	537–715	128
3	157	ttg tat act aaa cta ctt aat ttt ttt tag CCC ACT CAA CAG–CTT CTT CCA GTG gta aag att cag tta gtg gaa taa ctt cgt	AG/GT	716–872	NA
4	198	cat tca tgc ttg ttt tgt ttt gga ttt tag TAA GGA CAG TCC–CCC TTT TAG AAG gta agt gtc tta tcc att tca tag tct agt	AG/GT	873–1070	NA
5	184	cct taa gtt cat tat tct ttc cct cat tag GTT GTT TCC CAG–CAA ACA CCC AAG gta ccg atg gtc aaa ttt agt tgg tgt gtc	AG/GT	1071–1254	NA
6	113	tta gtg att aat att ttt ttt tta aat tag GTC TCT CTT GAT–ATT CAG TAA TGG gta agg att aga cgt tta ctt ttt agt acc	AG/GT	1255–1367	106
7	132	ctt act ttg tct tgt gat ttt tgt ttg cag GTC CTA AAT ATG–AAG AAT GTA AAG gta ttg tta ttt att tgt tta tga gga gat	AG/GT	1368–1499	NA
8	239	tag cat agt gac ttc att ttt ttt tta aag GCT CTC CCC TTG–GTG CCT ACA AAG gta atg gga tca atg atc ctc atc att ggg	AG/GT	1500–1738	399
9	168	ggc ata tta aat act tac aac aat tcc tag GTG TTA TGT ATT–AGC CAG CTT CAG gta ctt gca tct tgg ttt act ttt ttt ttt	AG/GT	1739–1906	NA
10	132	tgg ctt ctg aaa cgt ttc att ggg ttg cag GAT CTA CAT AAG–AAG ATG CAC AAG gta aga tga ccc att tgg aaa tac ttt tat	AG/GT	1907–2038	NA
11	114	gct gct gat act act ttt tgt ttt tta aag GAA CTT TGT GCT–CTA GAT GAA AAG gta tat ata tta aca tga aaa att agt gct	AG/GT	2039–2152	446
12	185	tgt tta taa gag att tca gtt tat ttg tag GAT TGT GCA GTC–CCT GGA ATG GAT gta agt agg tta gga gag aaa cca aag gga	AG/GT	2153–2337	NA
13	127	aat ttc tgt tca ttt ttt ccc tgt att tag AAA CAA AAA AAA–AAA ACC TTA CAG gta aaa cac atc tct tga gaa aaa tgc aaa	AG/GT	2338–2464	NA
14	126	ata aaa aat att tta ttg tta ctt gtg cag GTG TTC AAA GCT–AAA AAA GTG AAG gta gga aaa tct ttt cct ctt gag ttg taa	AG/GT	2465–2590	NA
15	132	att tgt aaa ttt ttt ctc ttt tct ctt tag ATT TGG AAT TCT–TGC TTC CTC AAA gta agt gtg gat att gag aat tag gta gat	AG/GT	2591–2722	NA
16	126	tta att tat ctt ttt ttg ttt cac aaa tag CTT TGG GAT TTG–GGA ACC TTA AAG gta tgc ttt tgt aca cta tta aaa tag ttg	AG/GT	2723–2848	NA
17	162	ctt ttt ctt ttt tat tac ttt aat tca aag CTT TGG GAT GCT–AAT AAA ATC TTT gta agt act tta aaa agc caa ctt cag tct	AG/GT	2849–3010	NA
18	129	cct tca tag gat ctc tat tta tgt tga cag CTT TTT GAC ATT–TAC TGT GTA GAG gtg agt agt tga att tat tct gtg aag cct	AG/GT	*	NA
19	126	gat ttc cta tat gct gtg ttt att ctg tag TTG TGG AAT ACA–CAG ACA ATC AGG gtg aga aat att gag att ttc att ttg aac	AG/GT	3011–3136	NA
20	120	gga atg ata att ttt tta tct ctt aat cag CTC TGG GAG ACA–AGA CGT CTG CAA gtg agt att ttt tag aaa aca att gga	AG/GT	3137–3256	NA
21	117	aat aac tga ttt tgc ctc att ttt cat tag CTC ATT AAT GGA–GGA GCC ATT GAG gta ttc agt gct agt ctt cag aat ctt tct	AG/GT	3257–3373	NA
22	126	ctt aat ttt gtg ggt ttt tct gct ttg aag ATT TTA GAA CTT–GCT GAA ATT CAG gtg aga ggg agg atg aac tct taa cat att	AG/GT	3374–3499	NA
23	120	tta taa cag act tat ttc ttt gat att cag GTA TGG AAT TGG–GGA ACA GTG AAG gta att taa agt ata aat ttg ttt ttt gaa	AG/GT	3500–3619	326
24	126	acc tcc aag tgt ttt ttt ttt ttt ttt aag GTA TGG AAT ATT–AAG ACT GCA AAG gta ggt caa tca att gaa acc atg cat aaa	AG/GT	3620–3745	355
25	126	cat tgc taa aca atc cta att gcc ttc cag ATC TGG AGT TTT–GGA GAA ATC AGG gta ggc tgt ttg ctg aca tga aag cac tgc	AG/GT	3746–3871	NA
26	144	gtt aat gaa ttg tgt atc atg ttt atg tag ATA TGG AAT GTC–GGA TAT ATT AAG gta aga gtt ccc caa gaa ctg tga aag aaa	AG/GT	3872–4015	NA
27	3007	cta atg aga att tta ttt ttc tct gaa cag TGG TGG AAC GTT–AAA ATT GTT TTG–	AG/–	4016–7022	

*Alternatively spliced exon derived from KIAA0413 sequence.

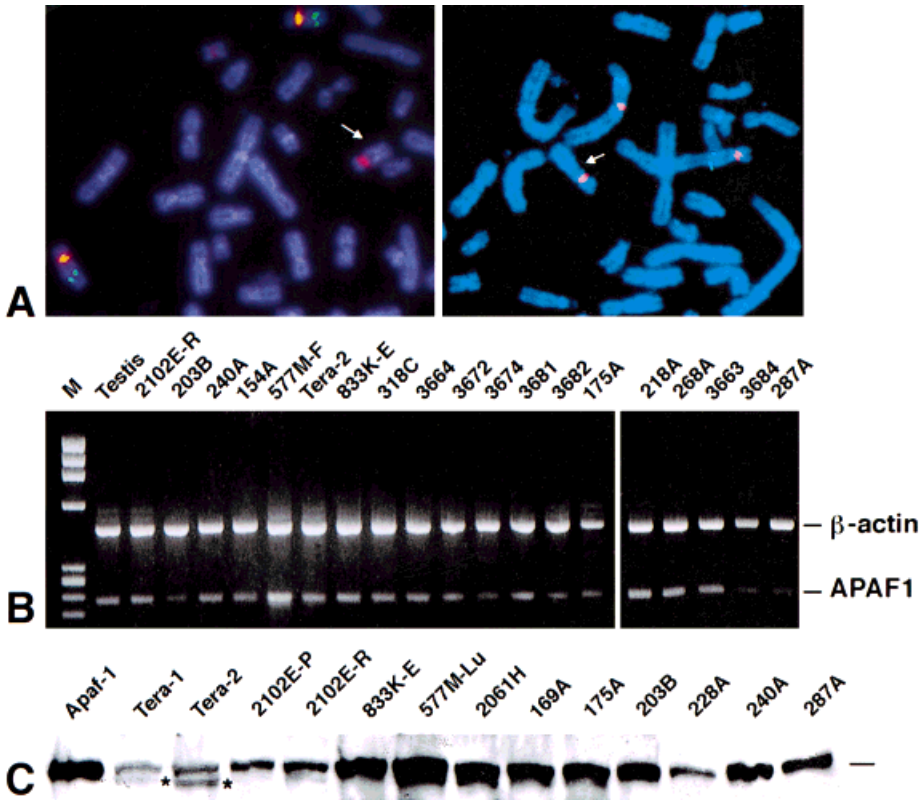

Figure 2. Genetic analysis of *APAF1*. (**A**) Identification of deletions at the 12q22 region containing *APAF1* gene using a PAC clone 373G19 as probe by double color FISH. Partial metaphases with DAPI counter stain showing centromeric (orange) and P379G19 (green) signals. Cell lines 218A (left) and 268A (right) with deleted chromosome 12 are indicated by arrows. (**B**) RT-PCR analysis of *APAF1* gene expression in GCTs. β-actin was used as an internal control. (**C**) Western blot analysis of APAF1. Aliquots of 100 μg lysates were subjected to 6% SDS-PAGE and electroblotted, and then the filters were probed with a polyclonal anti-Apaf-1 antibody (see Methods). APAF1 reactive bands were identified by comparing with the position of purified Apaf-1. The position of the APAF1 is indicated on the gel. Asterisks indicate aberrant-size bands.

analyzed showed signals only at 12q22 (data not shown). FISH analysis identified *APAF1* gene deletions in 2 of 8 (25%) GCT cell lines (268A, 218A), that exhibited fewer P373G19 signals compared to centromeric signals (Fig. 2A). To ascertain whether *APAF1* is a candidate TSG, RT-PCR using overlapping sets of primers spanning the entire coding region was performed, followed by SSCP analysis on 17 GCT cell lines and 10 primary tumors. No mutations were found.

Northern analysis of poly A^+ RNA was performed on 8 GCT cell lines hybridized with a cDNA probe to assess the levels of *APAF1* mRNA. No *APAF1* mRNA was detected in any cell line, whereas the control β-actin showed abundant expression, suggesting undetectable levels or lack of expression of *APAF1* mRNA in GCT cell lines (data not shown). To assess the *APAF1* expression further, 35 cycles of multiplex RT-PCR were performed on cDNA using primers spanning 2 different exons of the gene. All 12 cell lines and 6 primary tumors analyzed showed detectable levels of *APAF1* message (Fig. 2B).

APAF1 Protein Expression and Analysis of Its Activity by Caspase-3 Cleavage

To assess the levels of APAF1 protein, we performed Western blot analysis on 17 GCT cell lines using polyclonal antibody directed against the CED-4 domain of APAF1. All cell lines analyzed showed appropriate-size immunoreactive bands against APAF1 antibody, with a considerable variation in protein levels. The Tera-2 and Tera-1 cell lines showed an abnormal protein of smaller molecular weight (≈120 kD) in addition to a normal-size protein (Fig. 2C). That this variant represents an alternatively spliced form of *APAF1* has not been ruled out. Variant forms of alternatively spliced *APAF1* due to additional WD40 repeats have been reported in human (Hu et al., 1999; Zou et al., 1999)

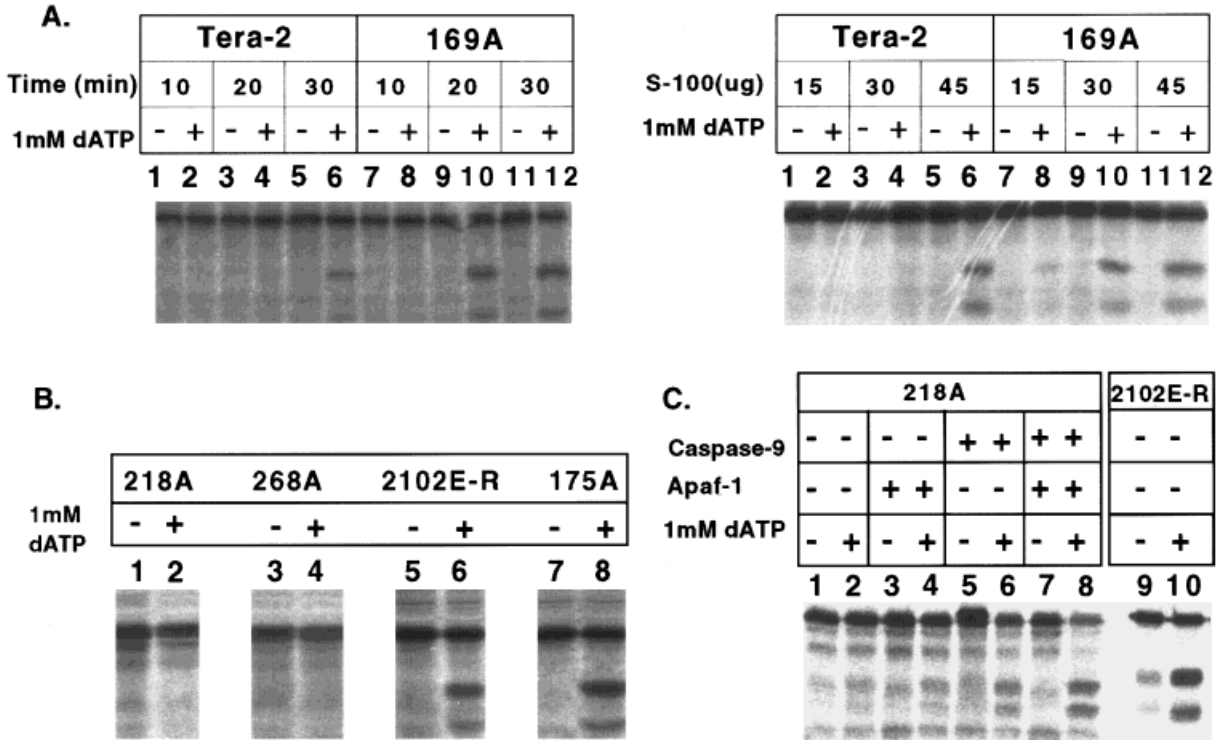

Figure 3. Analysis of dATP-dependent caspase-3 activation in GCT cell lines. (**A**) **Left panel**: aliquots (2 μl) of in vitro-translated, ^{35}S-labeled, and affinity-purified caspase-3 were incubated at 30°C for 1.5 hr with 10 μg (**lanes 1**, **2**, **7**, **8**), 20 μg (**3**, **4**, **9**, **10**) or 30 μg (**5**, **6**, **11**, **12**) of S-100 from Tera-2 or 169A cell lines. **Right panel**: aliquots (2 μl) of ^{35}S caspase-3 were incubated at 30°C with 30 μg of S-100 from Tera-2 or 169A cell lines for 15 min (lanes 1, 2, 7, 8), 30 min (3, 4, 9, 10) or 45 min (5, 6, 11, 12) in the presence (lanes 2, 4, 6, 8, 10, 12) or absence (lanes 1, 3, 5, 7, 9, 11) of 1 mM dATP and 1 mM $MgCl_2$ in a final volume of 32 μl. (**B**) Aliquots (2 μl) of in vitro-translated, ^{35}S-labeled, and affinity-purified caspase-3 were incubated at 30°C for 2.5 hr with 80 μg aliquots of GCT S-100 from cell lines 218A (lanes 1, 2), 268A (lanes 3, 4), 2102E-R (lanes 5, 6) or 175A (lanes 7, 8) in the presence (lanes 2, 4, 6, 8) or absence (lanes 1, 3, 5, 7) of 1 mM dATP and 1 mM $MgCl_2$ in a final volume of 32 μl. (**C**) Aliquots (2 μl) of in vitro-translated, ^{35}S-labeled, and affinity-purified caspase-3 were incubated at 30°C for 4 hr with 30 μg aliquots of S-100 from cell lines 218A (lanes 1–8) or 2102E-R (lanes 9, 10) supplemented with 200 ng of cytochrome c (Sigma) in the presence (lanes 2, 4, 6, 8, 10) or absence (lanes 1, 3, 5, 7, 9) of 1 mM dATP and 1 mM $MgCl_2$ in a final volume of 30 μl. Samples were additionally supplemented with either 300 ng of recombinant APAF1 (lanes 3, 4, 7, 8) or 65 ng of recombinant caspase-9 (lanes 5–8). In all experiments, after incubation, samples were subjected to 15% SDS-PAGE and transferred to nitrocellulose filters. The filters were exposed overnight to a phosphorimaging plate at room temperature.

as well as in mouse (Cecconi et al., 1998) cells. WD-40 repeats in APAF1 play a role in recruiting procaspase-3 to the APAF1-caspase-9 complex. Mutants carrying deletion in the WD-40 region fail to activate procaspase-3 and are deficient in apoptosis (Hu et al., 1999).

APAF1 functions to mediate the activation of caspase-3 in response to exposure to cytochrome c and dATP (Li et al., 1997; Zou et al., 1997). To examine whether 12q22 deletions in GCT affect APAF1 function, we assayed S-100 cytosolic extracts for dATP-induced cleavage of in vitro translated radio-labeled caspase-3 as a marker for APAF1 activity. Of seven GCT cell lines tested, three (Tera-2, 218A, and 268A) showed lack or decrease in dATP-mediated caspase-3 cleavage (Fig. 3A,B). In Tera-2, the cell line that showed the aberrant protein, the cell extract exhibited undetectable or no activity at low concentrations of S-100 (10 and 20 μg), and a detectable level of activity was seen only when large amounts of protein (30 μg) were used. In the other cell lines (169A, 2102E-R, and 175A), a high level of activity was detected with as little as 10 μg protein (Fig. 3A). The cell lines 268A and 218A showed no dATP-mediated APAF1 activity even after addition of large amounts of protein to the reaction mixture (80 μg for 268A and 120 μg for 218A) (Fig. 3B). This lack of APAF1 activity correlates with genetic deletions seen by FISH in the cell lines 268A and 218A.

To determine whether this lack or decreased caspase-3 activity was due to disruption of APAF1 protein expression, we performed Western blot analysis that confirmed the presence of appropriately sized immunoreactive bands in all of the cell extracts examined (Fig. 2B and data not shown). Because the activation of caspase-3 is dependent

on the presence of APAF1, cytochrome c, and caspase-9, these proteins were added back to S-100 to determine which components were deficient in the GCT cell lines that showed a lack of or decrease in activity. Figure 3C shows the results after supplementation of these protein components in cell extract from the 218A cell line. Similar results were obtained for 268A extracts (data not shown). Cytochrome c is abundantly present in the S-100 cytosolic fraction (Kim et al., 1997) and addition of cytochrome c had no effect on activation of dATP-dependent activity (Fig. 3C, lanes 1 and 2). Addition of recombinantly expressed APAF1 showed only a marginal increase in dATP activation of caspase-3 cleavage (Fig. 3C, lanes 3 and 4). Introduction of recombinant caspase 9 markedly increased the activity in the cell line (Fig. 3C, lanes 5 and 6). The activity of the recombinant protein is demonstrated by co-addition to the cell extract (Fig. 3C, lanes 7 and 8). These data indicate that the deficiency in caspase-3 activation in these extracts is not due to the absence of active APAF1 protein.

DISCUSSION

The 12q22 band has been suggested to harbor a potential TSG in male GCTs (Murty et al., 1990; Samaniego et al., 1990; Murty et al., 1992, 1996, 1999; Rodgriguez et al., 1992). The same region has also been shown to be frequently deleted in pancreatic carcinomas (Hahn et al., 1995; Kimura et al., 1996, 1998). These studies strongly implicated the presence of a TSG at 12q22. In an attempt at positional cloning of the candidate TSG, we mapped the *APAF1* gene immediately distal to the common region of deletion in GCTs. In view of the critical role played by the *APAF1* gene in the apoptotic pathway, we considered the gene as a strong candidate TSG for 12q22 deletions and examined its role in GCT. The initial FISH analysis identified *APAF1* deletions in 25% of GCT cell lines. These data provided evidence that the *APAF1* gene is within a deleted segment of 12q22 in a certain proportion of GCTs, thus leading to further analyses of the gene in these tumors. It has previously been shown that one of the cell lines (218A) exhibited LOH at 12q22 (Murty et al., 1996). Similarly, 57% (four of seven) pancreatic carcinoma cell lines analyzed also showed deletions of the *APAF1* gene (data not shown).

To find whether the *APAF1* gene functions as a TSG, we studied genetic and functional alterations of the gene in GCTs. Lack of mutations in *APAF1* suggested that the gene is not inactivated by mechanisms involving loss of function. We also have not found any mutations in 8 pancreatic carcinoma cell lines analyzed (data not shown). Consistent with this, we did not find any gross genomic alterations in the *APAF1* gene in 45 GCT DNAs studied by Southern blot analysis (data not shown). To examine the *APAF1* expression, we first examined mRNA by Northern analysis and could not find any detectable levels of expression in GCT cell lines. We then determined whether *APAF1* was expressed by RT-PCR and protein by Western blot analysis. Both mRNA and proteins were detected in all GCTs analyzed, including the Tera-2 cell line that exhibited an aberrant-sized protein.

To determine whether the genetic deletions and the variations in mRNA and protein affect the functional activity of APAF1, we assessed caspase-3 activation in GCT cell lines. We measured the activity of dATP-dependent, APAF1-mediated caspase-3 cleavage in the Tera-2 cell line, which showed an aberrant-sized protein, at various concentrations of S-100 with different incubation periods. Caspase-3 was not activated at low concentrations of protein and at shorter incubation periods with these cells, in contrast to marked cleavage of caspase-3 in other cell lines (e.g., 169A). Detectable caspase-3 cleavage was seen in Tera-2 only after addition of a high concentration of protein and prolonged incubation times. In two other GCT cell lines, 218A and 268A, that exhibited *APAF1* gene deletions, the dATP-dependent activation of caspase cleavage was found to be defective, without any detectable forms of active caspase-3 even at higher concentrations of protein with prolonged incubation periods (Fig. 3B). Utilizing similar conditions, the cell lines 2102E-R and 175A, that did not exhibit *APAF1* genomic deletions, showed markedly higher levels of caspase-3 cleavage. Hence, these data suggest that the cell lines 218A and 268A are defective in the dATP-dependent apoptotic pathway.

To determine whether this decrease or lack of active caspase-3 is due to relative levels of APAF1 or other components in the pathway, we added recombinant APAF1 and caspase-9 in these experiments. Addition of recombinant APAF1 did not restore caspase activation in cell line 218A (Fig. 3C). Identical results were obtained with the cell line 268A (results not shown). Recombinant APAF1 has been shown to promote the activation of caspase-3 in the presence of recombinant caspase-9 and pure cytochrome c or in by addition to Apaf-1 −/− fibroblast extracts (Zou et al., 1999). These data, thus, suggest that the defect is not due

to a disruption of the *APAF1* gene itself. This latent activity was best demonstrated by addition of purified recombinant caspase-9, that exhibited detectable active caspase-3 in the cell line 218A (Fig. 3C, lanes 5 and 6). Supplementation of caspase-9 with or without addition of APAF1 restored the caspase-3 cleavage, although a marked increase occurred when both components were added. Because the caspase-9 protein was detectable in all cell lines by Western analysis (data not shown), these data suggest that the defect in dATP-mediated caspase activation may be in an endogenous regulatory pathway or due to a dominant-negative form of APAF1 that might compete for caspase-9 recruitment. No evidence for dominant-negative mutations was found, however, by examination of the *APAF1* mRNA transcript in these cells by SSCP analysis. Whereas the defect is not directly due to a disruption of *APAF1* expression, the link between genomic deletions containing *APAF1* and the dATP activation of caspase cleavage is intriguing. These deletions may also point to the regulated inactivation of caspase-9 or perhaps other components of the *APAF1*-mediated pathway for caspase activation in response to disruption of another gene in the 12q22 deleted region tightly linked to the *APAF1* gene. It is now known that at least one other gene, *RAIDD* (Rip-associated ICH1/CED3-homologous protein with death domain), that controls apoptosis is mapped to the 12q22 region. The growth-factor-dependent regulation of BAD phosphorylation and the binding to Bcl-X demonstrate that such connections exist between cell cycle controls and apoptosis for other arms of the apoptotic control machinery (Datta et al., 1997; del Peso et al., 1997). Taken together, these data do not support a role for *APAF1* as a candidate TSG targeting 12q22 deletions in GCT. It remains to be seen, however, whether other mechanisms involving downstream genes in the pathway play a role in tumorigenesis in these tumors. The genomic structure of the *APAF1* gene generated in the present study would be of relevance in facilitating further studies in this direction in normal and disease states.

ACKNOWLEDGMENT

We thank Amelia Panico for help in preparing the figures.

REFERENCES

Cecconi F, Alvarez-Bolado G, Meyer BI, Roth KA, Gruss P. 1998. Apaf1 (CED-4 homolog) regulates programmed cell death in mammalian development. Cell 94:727–737.

Chaganti RSK, Murty VVVS, Bosl GJ. 1996. Molecular genetics of male germ cell tumors. In: Vogelzang NJ, Scardino PT, Shipley WU, Coffey DS, editors. Comprehensive textbook of genitourinary oncology. Baltimore: Williams & Wilkins. p 932–940.

Datta SR, Dudek H, Tao X, Masters S, Fu H, Gotoh Y, Greenberg ME. 1997. Akt phosphorylation of BAD couples survival signals to the cell-intrinsic death machinery. Cell 91:231–241.

del Peso L, Gonzalez-Garcia M, Page C, Herrera R, Nunez G. 1997. Interleukin-3-induced phosphorylation of BAD through the protein kinase Akt. Science 278:687–689.

Dib C, Faure S, Fizames C, Samson D, Drouot N, Vignal A, Millasseau P, Marc S, Hazan J, Seboun E, Lathrop M, Gyapay G, Morissette J, Weissenbach J. 1996. A comprehensive genetic map of the human genome based on 5,264 microsatellites. Nature 380:152–154.

Fey MF, Hesketh C, Wainscoat JS, Gendler S, Thein SL. 1989. Clonal allele loss in gastrointestinal cancers. Br J Cancer 59:750–754.

Hahn SA, Seymour AB, Hoque ATMS, Schutte M, da Costa LT, Redston MS, Caldas C, Weinstein CL, Fischer A, Yeo CJ, Hruban RH, Kern SE. 1995. Allelotype of pancreatic adenocarcinoma using xenograft enrichment. Cancer Res 55:4670–4675.

Horvitz HR. 1999. Genetic control of programmed cell death in the nematode *Caenorhabditis elegans*. Cancer Res 59(Suppl):1701S–1706S.

Houldsworth J, Reuter V, Bosl GJ, Chaganti RSK. 1997. Aberrant expression of cyclin D2 is an early event in human male germ cell tumorigenesis. Cell Growth Differ 8:293–299.

Hu Y, Benedict MA, Wu D, Inohara N, Nunez G. 1998. Bcl-XL interacts with Apaf-1 and inhibits Apaf-1-dependent caspase-9 activation. Proc Natl Acad Sci USA 95:4386–4391.

Hu Y, Benedict MA, Ding L, Nunez G. 1999. Role of cytochrome c and dATP/ATP hydrolysis in apaf-1-mediated caspase-9 activation and apoptosis. EMBO J 18:3586–3595.

Janicke RU, Sprengart ML, Wati MR, Porter AG. 1998. Caspase-3 is required for DNA fragmentation and morphological changes associated with apoptosis. J Biol Chem 273:9357–9360.

Kim CN, Wang X, Huang Y, Ibrado AM, Liu L, Fang G, Bhalla K. 1997. Overexpression of Bcl-X(L) inhibits Ara-C-induced mitochondrial loss of cytochrome c and other perturbations that activate the molecular cascade of apoptosis. Cancer Res 57:3115–3120.

Kimura M, Abe T, Sunamura M, Matsumo S, Horii A. 1996. Detailed deletion mapping on chromosome arm 12q in human pancreatic adenocarcinoma: identification of a I-cM region of common allelic loss. Genes Chromosomes Cancer 17:88–93.

Kimura M, Furukawa T, Abe T, Yatsuoka T, Youssef EM, Tokoyama T, Ouyang H, Ohnishi Y, Sunamura M, Kobari M, Matsuno S, Horii A. 1998. Identification of two common regions of allelic loss in chromosome arm 12q in human pancreatic cancer. Cancer Res 58:2456–2460.

Kucherlapati R, Marynen P, Turc-Carel C. 1997. Report of the Fourth International Workshop on Human Chromosome 12 Mapping 1997. Cytogenet Cell Genet 78:82–95.

Li P, Nijhawan D, Budihardjo I, Srinivasulu SM, Ahmad M, Alnemri ES, Wang X. 1997. Cytochrome c and dATP-dependent formation of Apaf-1/caspase-9 complex initiates an apoptotic protease cascade. Cell 91:479–489.

Liu X, Kim CN, Yang J, Jemmerson R, Wang X. 1996. Induction of apoptotic program in cell-free extracts: requirement for dATP and cytochrome c. Cell 86:147–157.

Murty VVVS, Dmitrovsky E, Bosl GJ, Chaganti RSK. 1990. Nonrandom chromosome abnormalities in testicular and ovarian germ cell tumor cell lines. Cancer Genet Cytogenet 50:67–73.

Murty VVVS, Houldsworth J, Baldwin S, Reuter V, Hunziker W, Besmer P, Bosl G, Chaganti RSK. 1992. Allelic deletions in the long arm of chromosome 12 identify sites of candidate tumor suppressor genes in male germ cell tumors. Proc Natl Acad Sci USA 89:11006–11010.

Murty VVVS, Li R-G, Houldsworth J, Bronson DL, Reuter VE, Bosl GJ, Chaganti RSK. 1994. Frequent allelic deletions and loss of expression characterize the DCC gene in male germ cell tumors. Oncogene 9:3227–3231.

Murty VVVS, Renault B, Falk CT, Bosl GJ, Kucherlapati R, Chaganti RSK. 1996. Physical mapping of a commonly deleted region, the site of a candidate tumor suppressor gene, at 12q22 in human male germ cell tumors. Genomics 35:562–570.

Murty VVVS, Montgomery K, Dutta S, Bala S, Renault B, Bosl GJ, Kucherlapati R, Chaganti RSK. 1999. A 3-Mb high-resolution BAC/PAC contig of 12q22 encompassing the 830-kb consensus

minimal deletion in male germ cell tumors. Genome Res 9:662–671.
Pan G, O'Rourke K, Dixit VM. 1998. Caspase-9, Bcl-XL, and Apaf-1 form a ternary complex. J Biol Chem 273:5841–5845.
Rodriguez E, Mathew S, Reuter V, Ilson DH, Bosl GJ, Chaganti RSK. 1992. Cytogenetic analysis of 124 prospectively ascertained male germ cell tumors. Cancer Res 52:2285–2291.
Samaniego F, Rodriguez E, Houldsworth H, Murty VVVS, Ladanyi M, Lele KP, Chen Q, Dmitrovsky E, Geller NL, Reuter V, Jhanwar SC, Bosl GJ, Chaganti RSK. 1990. Cytogenetic and molecular analysis of human male germ cell tumors: chromosome 12 abnormalities and gene amplification. Genes Chromosomes Cancer 1:289–300.
Schneider BG, Pulitzer DR, Brown RD, Prihoda TJ, Bostwick DG, Saldivar V, Rodriguez-Martinez HA, Gutierrez-Diaz MEC, O'Connel P. 1995. Allelic imbalance in gastric cancer: an affected site on chromosome arm 3p. Genes Chromosomes Cancer 13:263–271.
Seymour A, Hruban RH, Redston M, Caldas C, Powell SM, Kinzler KW, Yeo CJ, Kern SE. 1994. Allelotype of pancreatic adenocarcinoma. Cancer Res 54:2761–2764.
Soengas MS, Alarcon RM, Yoshida H, Giaccia AJ, Hakem R, Mak TK, Lowe SW. 1999. Apaf-1 and caspase-9 in p53-dependent apoptosis and tumor inhibition. Science 284:156–159.
Yang X, Chang HY, Baltimore D. 1998. Essential role of CED-4 oligomerization in CED-3 activation and apoptosis. Science 281: 1355–1357.
Yoshida H, Kong Y-Y, Yoshida R, Elia AJ, Hakem A, Hakem R, Penninger JM, Mak TW. 1998. Apaf1 is required for mitochondrial pathways of apoptosis and brain development. Cell 94:739–750.
Zou H, Henzel WJ, Liu X, Lutschg A, Wang X. 1997. Apaf-1, a human protein homologous to *C. elegans* CED-4, participates in cytochrome c-dependent activation of caspase-3. Cell 90:405–413.
Zou H, Li Y, Liu X, Wang X. 1999. An APAF-1.cytochrome c multimeric complex is a functional apoptosome that activates procaspase-9. J Biol Chem 274:11549–11556.